Failed excitonic quantum phase transition in $Ta_2Ni(Se_{1-x}S_x)_5$

Pavel A. Volkov,[1,*] Mai Ye,[1,†] Himanshu Lohani,[2] Irena Feldman,[2] Amit Kanigel,[2] and Girsh Blumberg[1,3,‡]

[1] *Department of Physics and Astronomy, Rutgers University, Piscataway, NJ 08854, USA*
[2] *Department of Physics, Technion - Israel Institute of Technology, Haifa 32000, Israel*
[3] *National Institute of Chemical Physics and Biophysics, 12618 Tallinn, Estonia*

(Dated: April 16, 2021)

We study the electronic phase diagram of the excitonic insulator candidates $Ta_2Ni(Se_{1-x}S_x)_5$ [x=0, ... ,1] using Raman spectroscopy. Critical excitonic fluctuations are observed, that diminish with x and ultimately shift to high energies, characteristic of a quantum phase transition. Nonetheless, a symmetry-breaking transition at finite temperatures is detected for all x, exposing a cooperating lattice instability that takes over for large x. Our study reveals a failed excitonic quantum phase transition, masked by a preemptive structural order.

Introduction: One of the fascinating manifestations of interactions between electrons in solids is the emergence of electronic orders. The fluctuations close to the respective quantum critical points are also believed to be the drivers of a wealth of yet unexplained behaviors, including strange metallicity and high-T_c superconductivity [1–4]. In many cases (such as, e.g., nematic [5, 6] or density-wave [7, 8] orders) electronic order breaks the symmetries of the crystalline lattice and the corresponding transitions can be, symmetry-wise, identical to structural ones. This raises the question of the role of the interplay between electronic and lattice degrees of freedom in the ordering. Even in cases where the lattice only weakly responds to the transition [9, 10], the critical temperatures [11, 12] and quantum critical properties [13] can be strongly modified. Moreover, in a number of cases the origin of the order is still under debate [14–16], as the lattice may develop an instability of its own.

The electronic-lattice dichotomy has recently come to the fore in studies of Ta_2NiSe_5 [17–19] - one of the few candidate material for the excitonic insulator (EI) phase [16, 20–24]. EI results from a proliferation of excitons driven by Coulomb attraction between electrons and holes in a semiconductor or a semimetal [25–29]. Ta_2NiSe_5 exhibits a phase transition at $T_c = 328\,\mathrm{K}$; while the pronounced changes in band structure [18], transport [19] and optical [30] properties are consistent with the ones expected for an EI, they allow an alternative interpretation in terms of a purely structural phase transition [31–33]. Indeed, EI state in Ta_2NiSe_5 is expected to break mirror symmetries of the lattice due to the distinct symmetries of the electron and hole states forming the exciton [34], similar to a structural transition [31]. Intriguingly, substitution of Se with S has been shown to suppress T_c in transport experiments to zero [19], suggesting a possible quantum phase transition (QPT) at $x = x_c$ in $Ta_2Ni(Se_{1-x}S_x)_5$. Increasing x enhances the band gap in the electronic structure [35], which is known to suppress the EI [27, 28], consistent with an EI QPT. On the other hand, the lattice degrees of freedom also evolve with x making it imperative to separately assess the roles of electronic and lattice degrees of freedom throughout the phase diagram of $Ta_2Ni(Se_{1-x}S_x)_5$. A promising technique to address this challenge is to probe the critical dynamics with polarization-resolved Raman scattering [36–38], that also allows to detect symmetry breaking independently [39–41].

In this Letter, we use polarization-resolved Raman scattering to study the dynamics of electronic excitations throughout the phase diagram of $Ta_2Ni(Se_{1-x}S_x)_5$. We reveal the presence of low-energy excitonic modes that soften on cooling towards $T_c(x)$ and deduce an excitonic transition temperature $T_{ex}(x) < T_c(x)$. On increasing sulfur content x, $T_{ex}(x)$ is suppressed to negative values and for $x = 1$ low-energy excitons are no longer observed, as expected for an excitonic insulator quantum phase transition. However, the actual $T_c(x)$ remains finite for all x, implying the presence of a cooperating lattice instability, obscuring the suppression of the excitonic order. The study thus reveals a "failed" excitonic quantum phase transition in $Ta_2Ni(Se_{1-x}S_x)_5$ masked by a preemptive structural order, that takes over as the electronic instability is suppressed.

Experimental: We performed Raman scattering experiments on four $Ta_2Ni(Se_{1-x}S_x)_5$ samples with varying Se/S content grown using the chemical vapor transport (CVT) method [42]. The measurements were performed in a quasi-back-scattering geometry on samples cleaved to expose the *ac* crystallographic plane with the 647 nm line from a Kr^+ ion laser excitation, details presented in Ref. [42]. The selection rules in the high-temperature orthorhombic (point group D_{2h}) phase imply that *ac* polarization geometry probes excitations with B_{2g} symmetry (same as that of the order parameter), while *aa* geometry probes the fully symmetric A_g ones [36–38, 42]. Below T_c, the point group symmetry is reduced to C_{2h} and the two irreducible representations merge, such that excitations from *ac* geometry above T_c may appear in *aa* geometry and vice versa. Their appearance allows to determine T_c from the Raman spectra.

Data overview: Summarized temperature dependence of the Raman susceptibility $\chi''(\omega, T)$ is presented in Fig. 1. The samples with $x = 0, 0.25, 0.67$ show qualitatively similar spectra. At low energies, phonon peaks

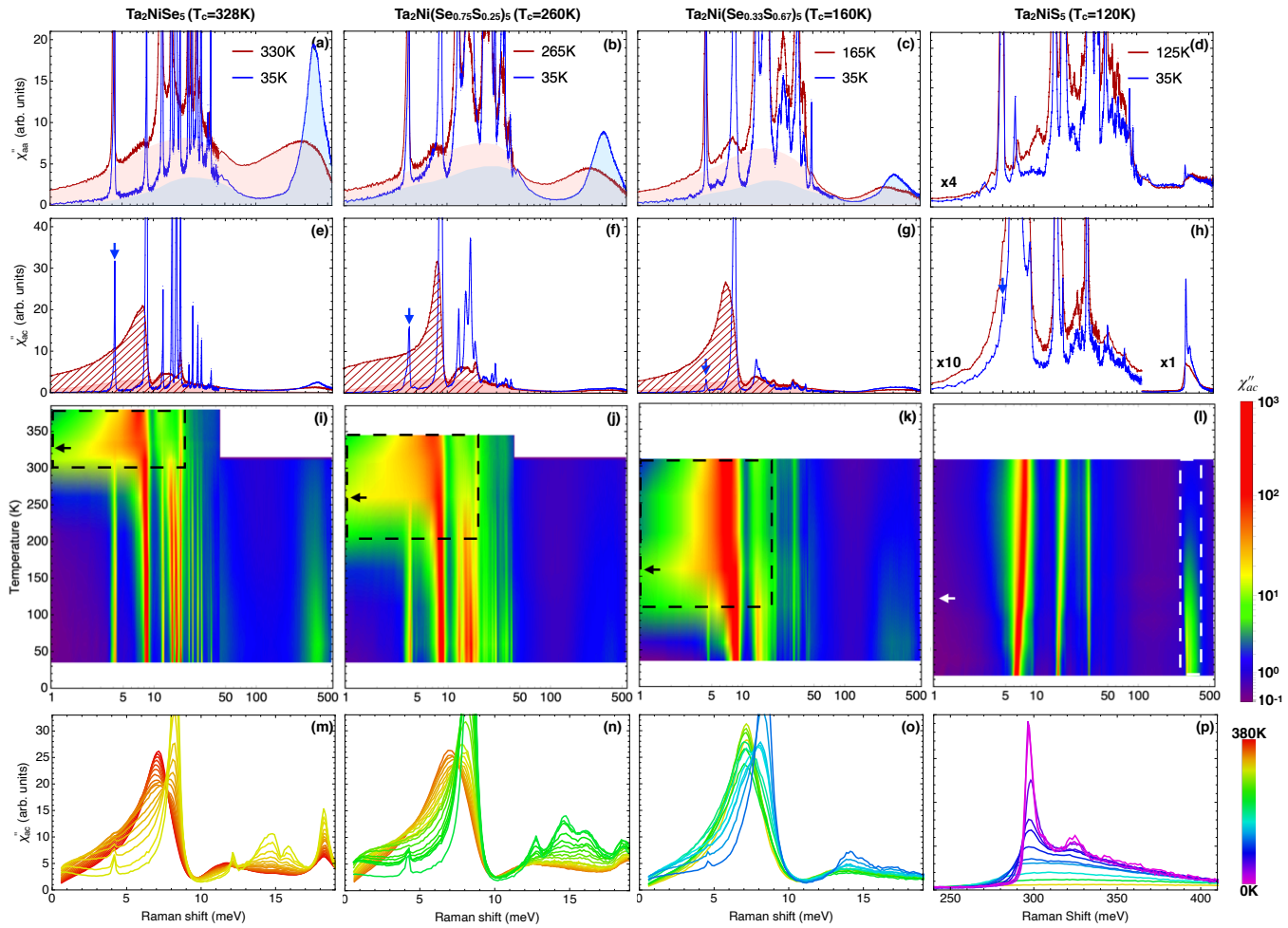

FIG. 1. Overview of the polarization-resolved Raman response $\chi''(\omega, T)$ in $Ta_2Ni(Se_{1-x}S_x)_5$. (a-d) Response in aa polarization geometry corresponding to fully symmetric (A_g) excitations above (red) and below (blue) T_c for $x = 0 - 1$. Shading highlights the bare electronic contribution to the response. (e-f) Same for ac geometry, probing the excitations with the symmetry of the order parameter (B_{2g}) for $T > T_c$ (red). Unlike aa geometry, phonons show an extremely anisotropic Fano lineshape (hatching), indicating their strong interaction with the electronic continuum (red shading). For $T < T_c$ (blue) excitations observed in aa geometry above T_c appear (arrow) due to symmetry breaking. (i-l) Temperature dependence of $\chi''_{ac}(\omega, T)$; an enhancement at low energies near T_c (arrow) is observed for $x = 0, 0.25, 0.67$. For $x = 1$ no low-energy response is present. (m-p) Details of $\chi''_{ac}(\omega, T)$ for regions marked by dashed lines in (i-k). (m-o) Fano lineshape of low-energy phonons due to interaction with electronic continuum. (p) High-energy peak due to an uncondensed exciton in Ta_2NiS_5 .

are observed on top of a smooth background, which we attribute to electronic excitations. On cooling, a pronounced redistribution of electronic intensity in a wide range of energies is observed, leading to a formation of a gap-like suppression followed by a high-energy peak Fig. 1(a)-(c). This peak at 380 meV for Ta_2NiSe_5 has been attributed to the coherence factors at the gap edge of an EI [36]. In ac geometry, a pronounced enhancement at low energies is evident close to T_c, consistent with critical mode softening near a second-order phase transition, Fig. 1(i)-(k). In the same temperature region, the lineshapes of the low-energy phonons show strongly asymmetric Fano form (Fig. 1(m)-(o)) - a known signature of interaction with an electronic excitation continuum [36, 42, 43]. This indicates the presence of low-energy symmetry-breaking electronic excitations, that soften close to T_c. At low temperatures, the asymmetry disappears (Fig. 1(e)-(g)), a behavior consistent with a gap opening in an EI. On increasing sulfur content x, the temperature where the strongest low-energy enhancement is observed progressively lowers (Fig. 1(i)-(k)), and the A_g-symmetry peak at about 380 meV becomes less pronounced and moves slightly to lower energy.

The signatures for Ta_2NiS_5 ($x = 1$) are rather different: in the ac geometry, no signatures of low-energy electronic excitations are visible at all temperatures, indicating the presence of a direct gap. This implies that between $x = 0.67$ and $x = 1$ the electronic structure undergoes a Lifschitz transition from a semimetallic to an insulating one. The intensity in the aa geometry at low

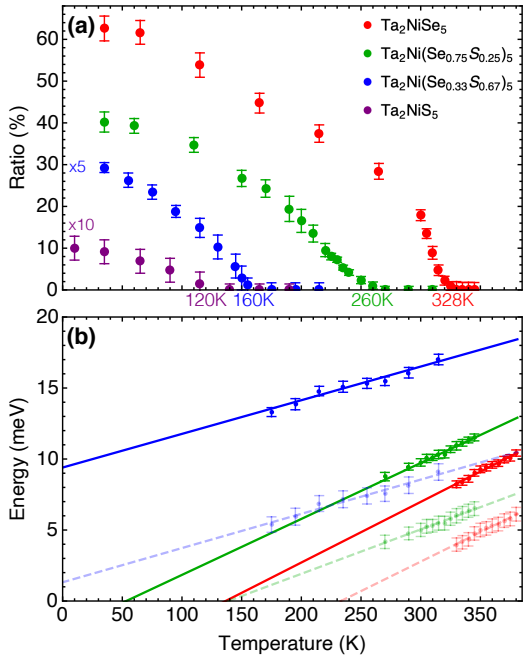

FIG. 2. The parameters deduced from the Raman response data, Fig. 1. (a) Integrated 'leakage' intensity into *ac* scattering geometries of the lowest-energy A_g phonon mode labeled in panels Fig. 1(e-h), normalized by the intensity in the dominant *aa* geometry. The mode's appearance in the *ac* scattering geometry below T_c implies the onset of symmetry breaking. (b) Bright points: Excitonic energy $\Omega_e(T)$, Eq. (1); Bleak points: the renormalized energy $\Omega_e^{comb}(T)$ including the exciton-phonon interaction obtained from the Fano fits to the lineshapes in Fig. 1. Lines represent linear fits to the points.

energies is also pronouncedly smaller then for the other samples and no broad high-energy peak is observed at low temperatures. On the contrary, a sharp feature at about 0.3 eV emerges in *ac* geometry on cooling below 100 K.

Symmetry-breaking transition: We address first the presence of a phase transition by studying the appearance of new modes in the broken-symmetry phase, as outlined above. In Fig. 2(a) we show the temperature dependence of such a 'leakage' phonon intensity marked by arrow in Fig. 1(e)-(h). One can see the appearance of the 'leaked' intensity below T_c in the pure Se case, as well as the decrease of T_c with S doping. At low x the obtained values of T_c agree with the ones deduced from transport and specific heat measurements [19, 42], Fig. 3. However, in contrast to the transport data reported in Ref. 19, we find that the symmetry-breaking transition persists for all compositions, although the 'leakage' intensity is strongly suppressed with higher x. The latter suggests that the phase transition signatures in thermodynamic and transport measurements may become too weak to be observed at large x, especially since the system becomes more insulating with x. The structural signatures, e.g. the deviation of the monoclinic angle β from 90°, should be also strongly suppressed, being already weak at $x = 0$ [17].

Electronic contribution to the phase transition: To elucidate the origin of the transition as a function of x, we investigate the soft-mode behavior observed for $x \leq 0.67$ (Fig. 1(i-k)). In particular, we analyze the asymmetric lineshapes of the low-energy part of $\chi''_{ac}(\omega, T)$ around T_c (Fig. 1(m-o)) using an extended Fano model [42]. The model assumes three phononic oscillators interacting with a continuum of excitonic origin. The latter is expected to arise from the excitonic fluctuations in a semimetal, overdamped due to the allowed decay into particle-hole pairs. The dynamics of the system is governed by the time-dependent Landau equations [44–47]:

$$\begin{aligned} \{\partial_t + \Omega_e(T)\}\varphi + \sum_{i=1}^{3} v_i \eta_i = 0, \\ \{\partial_t^2 + \gamma_i(T)\partial_t + \omega_{pi}^2(T)\}\eta_i + v_i \varphi = 0, \end{aligned} \tag{1}$$

where $\eta_{i=1,2,3}$ and φ are the collective coordinates (order parameters) of the optical phonons and excitons, respectively. $\Omega_e(T)$ is the characteristic energy of the excitonic fluctuations, $\omega_{pi}(T)$ and $\gamma_i(T)$ are the phonon frequencies and scattering rates, and a bilinear exciton phonon-coupling v_i is assumed. The linear response of the system Eq. (1) determines the Raman susceptibility. The resulting purely excitonic linear response function has then the form of a broad continuum $\chi''_{cont}(\omega, T) \propto \frac{\omega}{\Omega_e^2(T)+\omega^2}$, in contrast to the Lorentzian phonon peaks. The interaction between the phonons and the excitonic continuum leads to an asymmetric broadening of the peaks [42], allowing to capture the observed lineshapes in great detail [36, 42].

We now discuss the parameters deduced from the Fano model fits. The phonon frequencies $\omega_{pi}(T)$ do not soften near T_c [42], ruling out a zone-center phonon instability [31]. On the other hand, $\Omega_e(T)$ (Fig. 2(b), solid lines) consistently softens above T_c for all semimetallic samples. The linear temperature dependence $\Omega_e(T) \sim T - T_{ex}$ implies that a purely electronic transition would have taken place at $T_{ex} < T_c$ for $x = 0, 0.25$ (Fig. 3, blue symbols). The strongly negative T_{ex} for $x = 0.67$ indicates that the exciton softeninng alone would not have lead to a transition at this sulfur concentration.

The suppression of the excitonic instability with x is even more evident in Ta_2NiS_5, Fig. 1(d,h,i), where the low-energy electronic response is altogether absent due to a direct band gap [35]. Instead, we observe a sharp B_{2g}-symmetry mode at 0.3 eV, Fig. 1(p), consistent with an in-gap exciton. It is followed by a weaker feature at 0.325 eV and an intensity 'tail' at higher energies up to around 0.4 eV [48] A 'leakage' of these features is also observed in *aa* geometry due to symmetry breaking, Fig. 1(d). On heating, all the features broaden and eventually smear out above 100 K. The increase of the linewidth of the excitonic features can be attributed to the interaction with acoustic and optical phonons [49].

Lattice effects and the phase diagram: The presented observations show that the excitonic instability on its own cannot explain the occurence of a transition for samples with large x, calling for a more careful consideration of the lattice effects. First, the coupling of excitons with the otherwise inert optical phonons can increase the transition temperature. Indeed, a zero-energy solution of Eqs. (1) exists when $\Omega_e^{comb}(T) = \Omega_e(T) - \sum_i \frac{v_i^2}{\omega_{pi}^2(T)}$ becomes zero. The deduced $\Omega_e^{comb}(T)$ shown in Fig. 2(b), dashed lines, indeed softens to zero at a temperature $T_{comb}(x)$ higher than $T_{ex}(x)$, green points in Fig. 3. $T_{comb}(x = 0.67)$ is however still negative, while the actual T_c is 170 K. For Ta_2NiS_5 , where the soft excitons are absent, the optical phonon modes exhibit around 15% softening on cooling. However, their energies never soften below 6.5 meV, Fig. 1(l), ruling them out as the driving force of the transition for Ta_2NiS_5 [42].

The only remaining option is an instability of the acoustic modes in Ta_2NiS_5 , i.e. ferroelasticity [50], driven by softening of the B_{2g} shear modulus $C_{ac}(T)$. The acoustic modes are not observed in Raman due to their extremely low energies and weak coupling to light [42, 51]. The intrinsic softening of shear modulus also affects the excitonic-driven transition via linear coupling λ of φ to the strain tensor component ε_{ac} that leads to enhancement of transition temperature defined by $\Omega_e^{comb}(T_{comb}^{FE}) - \lambda^2/[2C_{ac}(T_{comb}^{FE})] = 0$, cf. Refs. [11, 12]. We capture $T_c(x)$ quantitatively assuming an x-independent Curie-Weiss softening of shear modulus $C_{ac}^{-1}(T) = C_{ac(0)}^{-1} + \frac{a}{T-120\text{K}}$, the black line in Fig. 3. Ignoring ferroelastic softening (i.e., taking $C_{ac}^{-1}(T) = C_{ac(0)}^{-1}$, the purple dashed line in Fig. 3) leads to a large deviation from actual $T_c(x)$ already at $x = 0.67$ and a complete suppression of ordering at $x_c \approx 0.8$.

This picture bears important consequences for the physics of $Ta_2Ni(Se_{1-x}S_x)_5$. At low x, the transition is driven, to a good approximation, only by the excitonic softening. On increasing x, the lattice softening becomes more important, and for $x = 1$ the transition is purely ferroelastic. In the absence of ferroelasticity, a lattice-shifted electronic QPT would have occurred at $x_c \approx 0.8$. While the presence of the lattice symmetry breaking at T_c suppresses the signatures of the QPT at low T, at temperatures higher than 120 K, the associated critical fluctuations are expected to appear [13]. The presence of quantum critical fluctuations due to a "failed" excitonic QPT lends a natural explanation to the signatures of strong correlations observed in Ta_2NiSe_5 . In particular, a filling-in, rather then closing of the gap in *aa* Raman spectra has recently been connected to strong electronic correlations [36]; moreover, ARPES studies [52] suggest the presence of "preformed excitons" well above T_c also characteristic of correlated regime. Similar temperature evolution of *aa* spectra is also observed for the doped samples, Fig. 1(b,c). Interestingly, while the intensity

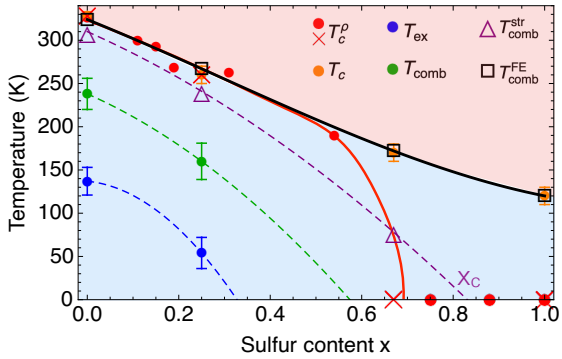

FIG. 3. Phase diagram of $Ta_2Ni(Se_{1-x}S_x)_5$. Orange points: the symmetry breaking transition temperature $T_c(x)$ obtained from the onset of phonon intensity 'leakage', Fig. 2(a). Red points and crosses: $T_c^\rho(x)$ adapted from transport studies Refs. [19, 42]. For low sulfur concentration x, the soft excitonic mode, Fig. 2(b), would drive the transition at temperature $T_{ex}(x)$ (blue points), that is enhanced to $T_{comb}(x)$ by coupling to inert optical phonons (green points), and is further enhanced to $T_{comb}^{str}(x)$ by coupling to the B_{2g} strain (purple triangles). For large x, the excitonic softening is suppressed, while a ferroelastic instability leads to a finite $T_{comb}^{FE}(x)$ (black squares). In the absence of the lattice instability, a lattice-shifted electronic QPT would have occurred at x_c (dashed purple line). Additionally, in the same proximity, the band structure undergoes semimetal-to-semiconductor Lifschitz transition (see text).

of the coherent *aa* peak is suppressed with doping, as is expected from mean-field theory [53], the position of the peak changes only weakly. The latter behavior indicates strong correlations which get a natural explanation in terms of the quantum critical fluctuations from the "failed" QPT. Finally, ferroelasticity may be suppressed by strain [54] or pressure [19] raising the possibility to reveal the bare EI QPT at low temperatures. As the Lifschitz transition occurs in the same range of x, the EI QPT may occur while system is still a semimetal, suggesting that secondary orders [55] or non-Fermi liquid physics may emerge.

Conclusions: In this work, we used polarized Raman scattering to reveal a "failed" excitonic insulator quantum phase transition at $x_c \approx 0.8$ in $Ta_2Ni(Se_{1-x}S_x)_5$, hidden by the onset of symmetry breaking due to a lattice instability. While at low sulfur content x we observed a soft excitonic mode driving the transition, at large x the mode ultimately transforms into a high-energy exciton, and only a cooperating ferroelastic instability is found to yield an explanation of the observed symmetry breaking transition. While the lattice instability masks the presence of the excitonic quantum phase transition, the associated critical fluctuations may still explain the correlation effects in Ta_2NiSe_5 at high temperatures. Furthermore, a controlled suppression of the structural instability by, strain [54] or pressure [19], can turn $Ta_2Ni(Se_{1-x}S_x)_5$ into a platform to study the excitonic QPT at low temperatures as well as quantum critical ferroeleasticity [56].

P.A.V and M.Y. contributed equally to this project. Authors acknowledge discussions with K. Haule. The spectroscopic work conducted at Rutgers was supported by NSF Grants No. DMR-1709161 (M.Y. and G.B). P.A.V. acknowledges the Postdoctoral Fellowship support from the Rutgers University Center for Materials Theory. The sample growth and characterization work conducted at the Technion was supported by the Israel Science Foundation Grant No. 320/17 (H.L., I.F. and A.K.). H.L. was supported in part by a PBC fellowship of the Israel Council for Higher Education. The work at NICPB was supported by the European Research Council (ERC) under Grant Agreement No. 885413.

* pv184@physics.rutgers.edu
† mye@physics.rutgers.edu
‡ girsh@physics.rutgers.edu

[1] H. v. Löhneysen, A. Rosch, M. Vojta, and P. Wölfle, Fermi-liquid instabilities at magnetic quantum phase transitions, Rev. Mod. Phys. **79**, 1015 (2007).
[2] M. Brando, D. Belitz, F. M. Grosche, and T. R. Kirkpatrick, Metallic quantum ferromagnets, Rev. Mod. Phys. **88**, 025006 (2016).
[3] D. J. Scalapino, A common thread: The pairing interaction for unconventional superconductors, Rev. Mod. Phys. **84**, 1383 (2012).
[4] T. Shibauchi, A. Carrington, and Y. Matsuda, A quantum critical point lying beneath the superconducting dome in iron pnictides, Annual Review of Condensed Matter Physics **5**, 113 (2014).
[5] S. A. Kivelson, E. Fradkin, and V. J. Emery, Electronic liquid-crystal phases of a doped mott insulator, Nature **393**, 550 (1998).
[6] E. Fradkin, S. A. Kivelson, M. J. Lawler, J. P. Eisenstein, and A. P. Mackenzie, Nematic fermi fluids in condensed matter physics, Annual Review of Condensed Matter Physics **1**, 153 (2010).
[7] G. Gruner, Density waves in solids (CRC press, 2018).
[8] S. A. Kivelson, I. P. Bindloss, E. Fradkin, V. Oganesyan, J. M. Tranquada, A. Kapitulnik, and C. Howald, How to detect fluctuating stripes in the high-temperature superconductors, Rev. Mod. Phys. **75**, 1201 (2003).
[9] J.-H. Chu, J. G. Analytis, K. De Greve, P. L. McMahon, Z. Islam, Y. Yamamoto, and I. R. Fisher, In-plane resistivity anisotropy in an underdoped iron arsenide superconductor, Science **329**, 824 (2010).
[10] R. M. Fernandes, A. V. Chubukov, and J. Schmalian, What drives nematic order in iron-based superconductors?, Nature Physics **10**, 97 (2014).
[11] J.-H. Chu, H.-H. Kuo, J. G. Analytis, and I. R. Fisher, Divergent nematic susceptibility in an iron arsenide superconductor, Science **337**, 710 (2012).
[12] A. E. Böhmer, P. Burger, F. Hardy, T. Wolf, P. Schweiss, R. Fromknecht, M. Reinecker, W. Schranz, and C. Meingast, Nematic Susceptibility of Hole-Doped and Electron-Doped $BaFe_2As_2$ Iron-Based Superconductors from Shear Modulus Measurements, Phys. Rev. Lett. **112**, 047001 (2014).
[13] I. Paul and M. Garst, Lattice effects on nematic quantum criticality in metals, Phys. Rev. Lett. **118**, 227601 (2017).
[14] R. Comin and A. Damascelli, Resonant x-ray scattering studies of charge order in cuprates, Annual Review of Condensed Matter Physics **7**, 369 (2016).
[15] D. Mou, A. Sapkota, H.-H. Kung, V. Krapivin, Y. Wu, A. Kreyssig, X. Zhou, A. I. Goldman, G. Blumberg, R. Flint, and A. Kaminski, Discovery of an Unconventional Charge Density Wave at the Surface of $K_{0.9}Mo_6O_{17}$, Phys. Rev. Lett. **116**, 196401 (2016).
[16] A. Kogar, M. S. Rak, S. Vig, A. A. Husain, F. Flicker, Y. I. Joe, L. Venema, G. J. MacDougall, T. C. Chiang, E. Fradkin, J. van Wezel, and P. Abbamonte, Signatures of exciton condensation in a transition metal dichalcogenide, Science **358**, 1314 (2017).
[17] F. D. Salvo, C. Chen, R. Fleming, J. Waszczak, R. Dunn, S. Sunshine, and J. A. Ibers, Physical and structural properties of the new layered compounds Ta_2NiS_5 and Ta_2NiSe_5, J. Less Common. Met. **116**, 51 (1986).
[18] Y. Wakisaka, T. Sudayama, K. Takubo, T. Mizokawa, M. Arita, H. Namatame, M. Taniguchi, N. Katayama, M. Nohara, and H. Takagi, Excitonic Insulator State in Ta_2NiSe_5 Probed by Photoemission Spectroscopy, Phys. Rev. Lett. **103**, 026402 (2009).
[19] Y. F. Lu, H. Kono, T. I. Larkin, A. W. Rost, T. Takayama, A. V. Boris, B. Keimer, and H. Takagi, Zero-gap semiconductor to excitonic insulator transition in Ta_2NiSe_5, Nat. Commun. **8**, 14408 (2017).
[20] J. Neuenschwander and P. Wachter, Pressure-driven semiconductor-metal transition in intermediate-valence $TmSe_{1-x}Te_x$ and the concept of an excitonic insulator, Phys. Rev. B **41**, 12693 (1990).
[21] K. Rossnagel, On the origin of charge-density waves in select layered transition-metal dichalcogenides, J. Phys. Condens. Matter **23**, 213001 (2011).
[22] L. Du, X. Li, W. Lou, G. Sullivan, K. Chang, J. Kono, and R.-R. Du, Evidence for a topological excitonic insulator in InAs/GaSb bilayers, Nat. Commun. **8**, 1971 (2017).
[23] Z. Li, M. Nadeem, Z. Yue, D. Cortie, M. Fuhrer, and X. Wang, Possible Excitonic Insulating Phase in Quantum-Confined Sb Nanoflakes, Nano Lett. **19**, 4960 (2019).
[24] Z. Zhu, P. Nie, B. Fauqué, B. Vignolle, C. Proust, R. D. McDonald, N. Harrison, and K. Behnia, Graphite in 90 T: Evidence for Strong-Coupling Excitonic Pairing, Phys. Rev. X **9**, 011058 (2019).
[25] L. V. Keldysh and Y. Kopaev, Sov. Phys. Solid State **6**, 2219 (1965).
[26] W. Kohn, Excitonic phases, Phys. Rev. Lett. **19**, 439 (1967).
[27] D. Jérome, T. M. Rice, and W. Kohn, Excitonic insulator, Phys. Rev. **158**, 462 (1967).
[28] B. I. Halperin and T. M. Rice, Possible anomalies at a semimetal-semiconductor transistion, Rev. Mod. Phys. **40**, 755 (1968).
[29] W. Kohn and D. Sherrington, Two kinds of bosons and bose condensates, Rev. Mod. Phys. **42**, 1 (1970).
[30] T. I. Larkin, A. N. Yaresko, D. Pröpper, K. A. Kikoin, Y. F. Lu, T. Takayama, Y.-L. Mathis, A. W. Rost, H. Takagi, B. Keimer, and A. V. Boris, Giant exciton Fano resonance in quasi-one-dimensional Ta_2NiSe_5, Phys. Rev. B **95**, 195144 (2017).
[31] A. Subedi, Orthorhombic-to-monoclinic transition in Ta_2NiSe_5 due to a zone-center optical phonon instabil-

ity, Phys. Rev. Materials **4**, 083601 (2020).
[32] M. D. Watson, I. Marković, E. A. Morales, P. Le Fèvre, M. Merz, A. A. Haghighirad, and P. D. C. King, Band hybridization at the semimetal-semiconductor transition of Ta_2NiSe_5 enabled by mirror-symmetry breaking, Phys. Rev. Research **2**, 013236 (2020).
[33] E. Baldini, A. Zong, D. Choi, C. Lee, M. H. Michael, L. Windgaetter, I. I. Mazin, S. Latini, D. Azoury, B. Lv, A. Kogar, Y. Wang, Y. Lu, T. Takayama, H. Takagi, A. J. Millis, A. Rubio, E. Demler, and N. Gedik, The spontaneous symmetry breaking in Ta_2NiSe_5 is structural in nature (2020), arXiv:2007.02909 [cond-mat.str-el].
[34] G. Mazza, M. Rösner, L. Windgätter, S. Latini, H. Hübener, A. J. Millis, A. Rubio, and A. Georges, Nature of symmetry breaking at the excitonic insulator transition: ta_2nise_5, Phys. Rev. Lett. **124**, 197601 (2020).
[35] Y. Chiba, T. Mitsuoka, N. L. Saini, K. Horiba, M. Kobayashi, K. Ono, H. Kumigashira, N. Katayama, H. Sawa, M. Nohara, Y. F. Lu, H. Takagi, and T. Mizokawa, Valence-bond insulator in proximity to excitonic instability, Phys. Rev. B **100**, 245129 (2019).
[36] P. A. Volkov, M. Ye, H. Lohani, I. Feldman, A. Kanigel, K. Haule, and G. Blumberg, Critical charge fluctuations and quantum coherent state in excitonic insulator Ta_2NiSe_5 (2020), arXiv:2007.07344 [cond-mat.str-el].
[37] K. Kim, H. Kim, J. Kim, C. Kwon, J. S. Kim, and B. J. Kim, Direct observation of excitonic instability in Ta_2NiSe_5, Nature Communications **12**, 1969 (2021).
[38] G. Blumberg, Comment on "Direct observation of excitonic instability in Ta_2NiSe_5", (2021), arXiv:2103.03073 [cond-mat.str-el].
[39] H.-H. Kung, R. Baumbach, E. Bauer, V. Thorsmølle, W.-L. Zhang, K. Haule, J. Mydosh, and G. Blumberg, Chirality density wave of the "hidden order" phase in URu_2Si_2, Science **347**, 1339 (2015).
[40] M. Ye, E. W. Rosenberg, I. R. Fisher, and G. Blumberg, Lattice dynamics, crystal-field excitations, and quadrupolar fluctuations of $YbRu_2Ge_2$, Phys. Rev. B **99**, 235104 (2019).
[41] S.-F. Wu, W.-L. Zhang, L. Li, H.-B. Cao, H.-H. Kung, A. S. Sefat, H. Ding, P. Richard, and G. Blumberg, Coupling of fully symmetric As phonon to magnetism in $Ba(Fe_{1-x}Au_x)_2As_2$, Phys. Rev. B **102**, 014501 (2020).
[42] M. Ye, P. A. Volkov, H. Lohani, I. Feldman, M. Kim, A. Kanigel, and G. Blumberg, Strongly interacting lattice dynamics in $Ta_2Ni(Se_{1-x}S_x)_5$ family of excitonic insulator, (2021), arXiv:2102.07912 [cond-mat.str-el].
[43] M. V. Klein, Electronic Raman Scattering, in Light Scattering in Solids I, Vol. 8, edited by M. Cardona (Springer-Verlag, Berlin, 1983) Chap. 4, pp. 147–202.
[44] N. Goldenfeld, Lectures on phase transitions and the renormalization group (CRC Press, 2018), .
[45] I. K. Schuller and K. E. Gray, Time-dependent ginzburg–landau: From single particle to collective behavior, Journal of Superconductivity and Novel Magnetism **19**, 401 (2006).
[46] R. Yusupov, T. Mertelj, V. V. Kabanov, S. Brazovskii, P. Kusar, J.-H. Chu, I. R. Fisher, and D. Mihailovic, Coherent dynamics of macroscopic electronic order through a symmetry breaking transition, Nature Physics **6**, 681 (2010).
[47] A. Zong, P. E. Dolgirev, A. Kogar, E. Ergeçen, M. B. Yilmaz, Y.-Q. Bie, T. Rohwer, I.-C. Tung, J. Straquadine, X. Wang, Y. Yang, X. Shen, R. Li, J. Yang, S. Park, M. C. Hoffmann, B. K. Ofori-Okai, M. E. Kozina, H. Wen, X. Wang, I. R. Fisher, P. Jarillo-Herrero, and N. Gedik, Dynamical slowing-down in an ultrafast photoinduced phase transition, Phys. Rev. Lett. **123**, 097601 (2019).
[48] The high-energy intensity 'tail' can be attributed to the interband transitions, while the second peak can be either a signature of the Rydberg series or strong exciton-phonon coupling.
[49] S. Rudin and T. L. Reinecke, Temperature-dependent exciton linewidths in semiconductor quantum wells, Phys. Rev. B **41**, 3017 (1990).
[50] E. K. Salje, Ferroelastic materials, Annual Review of Materials Research **42**, 265 (2012).
[51] Y. Gallais and I. Paul, Charge nematicity and electronic raman scattering in iron-based superconductors, Comptes Rendus Physique **17**, 113 (2016).
[52] K. Seki, Y. Wakisaka, T. Kaneko, T. Toriyama, T. Konishi, T. Sudayama, N. L. Saini, M. Arita, H. Namatame, M. Taniguchi, N. Katayama, M. Nohara, H. Takagi, T. Mizokawa, and Y. Ohta, Excitonic Bose-Einstein condensation in Ta_2NiSe_5 above room temperature, Phys. Rev. B **90**, 155116 (2014).
[53] In a two-band model of EI $\chi''_a a(\omega) \sim \nu_0\sqrt{2W/(\omega-2W)}$ [36], where ν is the density of states above T_c and W is the interband hybridization, which is the order parameter for pure EI [34].
[54] M. S. Ikeda, T. Worasaran, J. C. Palmstrom, J. A. W. Straquadine, P. Walmsley, and I. R. Fisher, Symmetric and antisymmetric strain as continuous tuning parameters for electronic nematic order, Phys. Rev. B **98**, 245133 (2018).
[55] P. A. Volkov and S. Moroz, Coulomb-induced instabilities of nodal surfaces, Phys. Rev. B **98**, 241107 (2018).
[56] M. Zacharias, I. Paul, and M. Garst, Quantum critical elasticity, Phys. Rev. Lett. **115**, 025703 (2015).